microbial biotechnology

Open Access

Engineering a probiotic strain of *Escherichia coli* to induce the regression of colorectal cancer through production of 5-aminolevulinic acid

Junhao Chen,[1] Xiaohong Li,[1] Yumei Liu,[1]
Tianyuan Su,[2] Changsen Lin,[3] Lijun Shao,[1]
Lanhua Li,[1] Wanwei Li,[1] Guoyu Niu,[1] Jing Yu,[3]
Ling Liu,[1] Miaomiao Li,[1] Xiaoli Yu[1] (ID) and
Qian Wang[2]

[1]School of Public Health, Weifang Medical University, Weifang, Shandong, 261053, China.
[2]State Key Laboratory of Microbial Technology, National Glycoengineering Research Center, Shandong University, Qingdao, Shandong, 266237, China.
[3]Affiliated Hospital of Shandong University of Traditional Chinese Medicine, Jinan, Shandong, 250014, China.

Summary

Bacterial vectors can be engineered to generate microscopic living therapeutics to produce and deliver anticancer agents. *Escherichia coli* Nissle 1917 (Nissle 1917) is a promising candidate with probiotic properties. Here, we used Nissle 1917 to develop a metabolic strategy to produce 5-aminolevulinic acid (5-ALA) from glucose as 5-ALA plays an important role in the photodynamic therapy of cancers. The coexpression of *hemA*^M and *hemL* using a low copy-number plasmid led to remarkable accumulation of 5-ALA. The downstream pathway of 5-ALA biosynthesis was inhibited by levulinic acid (LA). Small-scale cultures of engineered Nissle 1917 produced 300 mg l^{-1} of 5-ALA. Recombinant Nissle 1917 was applied to deliver 5-ALA to colorectal cancer cells, in which it induced the accumulation of antineoplastic protoporphyrin X (PpIX) and specific cytotoxicity towards colorectal cancer cells irradiated with a 630 nm laser. Moreover, this novel combination therapy proved effective in a mouse xenograft model and was not cytotoxic to normal tissues. These findings suggest that Nissle 1917 will serve as a potential carrier to effectively deliver 5-ALA for cancer therapy.

Introduction

Genetically engineered microbes effectively synthesize biologically active molecules such as antigens, enzymes and vitamins (Pedrolli *et al.*, 2019). Moreover, bacteria produce numerous therapeutic compounds such as 5-aminolevulinic acid (5-ALA) (Yu *et al.*, 2015). Certain live microorganisms, which are defined as probiotics, confer a health benefit upon the host when administered in adequate amounts (Hill *et al.*, 2014). Combination of the productive and probiotic features of microbes into living therapeutics is a new era in probiotic research (Singh *et al.*, 2017).

Probiotic organisms are mainly isolated from the gut or from traditional fermented foods. As a living delivery system, *Escherichia coli* (*E. coli*) offers the advantage of its high prevalence in the human gut. Numerous biological approaches are available for metabolic engineering of *E. coli*, indicating that *E. coli* provides an optimal platform for creating living therapeutics (Pedrolli *et al.*, 2019).

A live microbe delivers constant concentrations of therapeutics to treat chronic diseases such as cancer, and their unique capabilities are well suited as ideal anti-cancer agents (Forbes, 2010). Among nonpathogenic *E. coli* strains, Nissle 1917 exhibits tumour-targeting activity and is a better choice for this purpose because of its probiotic potential (Piñero-Lambea *et al.*, 2015; Chua *et al.*, 2017). The complete genomic sequence of Nissle 1917 makes possible the identification of genes and their products that are essential for its probiotic nature (Reister *et al.*, 2014). This knowledge is used to effectively manipulate Nissle 1917 for therapeutic applications. For example, Nissle 1917 can be engineered to produce therapeutic proteins and prodrug-converting enzymes, which reduce tumour volume and increase survival in animal models, while avoiding damage to healthy cells (Yu *et al.*, 2020). Moreover, Nissle 1917 was engineered to express a synchronized lysis circuit (eSLC) to locally release an encoded nanobody antagonist of CD47 (eSLC-CD47nb). The local delivery of immunotherapeutic payloads by Nissle 1917 achieves systemic antitumor immunity (Chowdhury *et al.*, 2019). We therefore selected Nissle 1917 as a carrier to deliver 5-aminolevulinic acid (5-ALA) to solid cancers.
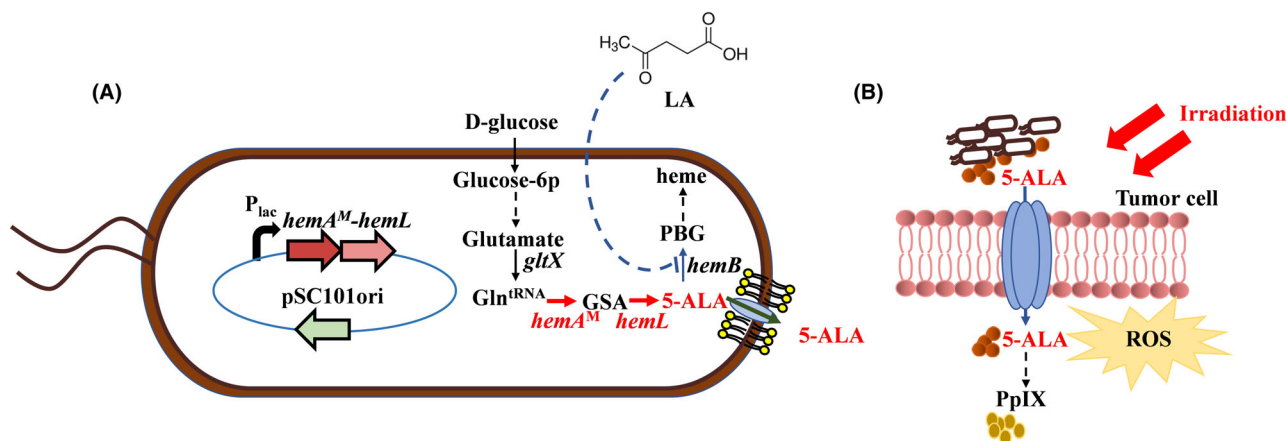
Fig. 1. 5-ALA production from glucose in Nissle 1917 (A) and targeted delivery of 5-ALA into tumour cells (B). 5-ALA, 5-aminolevulinic acid; GSA, glutamate-1-semialdehyde aminotransferase; Gln^{tRNA}, glutamyl-tRNA; LA, levulinic acid; PBG, porphobilinogen; PpIX, protoporphyrin IX; ROS, reactive oxygen species.

5-ALA, a natural amino acid, is a key intermediate in the biosynthesis of tetrapyrrole (Schauer *et al.*, 2002). It attracts considerable attention because of its potential applications for localizing tumours and as a component of photodynamic therapy (PDT) of cancers such as colorectal cancer, which ranks third in incidence and second in mortality (Woźniak *et al.*, 2015; Bray *et al.*, 2018). Protoporphyrin IX (PpIX), which is converted from 5-ALA, is a highly efficacious photosensitizing agent employed for PDT (Kim *et al.*, 2013). Excitation of a photosensitizer by irradiation with a suitable light source (400–750 nm) produces significant amounts of reactive oxygen species (ROS), which damage DNA and cell membranes through lipid peroxidation and alteration of membrane fluidity. Damage to cellular organelles is harnessed to kill tumour cells (Sharma *et al.*, 2007). Furthermore, 5-ALA-PDT achieves high selectivity for targeting tumours because of the preferential accumulation of photosensitizers in tumours, and therefore serves as a standard cancer therapy (Dougherty *et al.*, 1998; Fujino *et al.*, 2016).

However, the high hydrophilicity of 5-ALA hinders its penetration into the hydrophobic interior of cell membranes, which is an obstacle to its clinical use (Donnelly *et al.*, 2008). Numerous methods such as coupling 5-ALA to a carrier have been explored to overcome this barrier (Yang *et al.*, 2009; Wu *et al.*, 2017). To address this problem, here we combined the biosynthetic and tumour-targeting features of the probiotic Nissle 1917 with PDT to deliver 5-ALA to colorectal cancer cells. For this purpose, Nissle 1917 was engineered to produce 5-ALA by applying pCL1920 to overexpress *hemA* and *hemL*. The secreted 5-ALA was delivered by Nissle 1917 to colorectal cancer cells to inhibit growth (Fig. 1). We propose its use as a new component of a tumour-targeting delivery system for cancer therapy.

Results

Engineering Nissle 1917 to produce 5-ALA

5-ALA biosynthesis in *E. coli* proceeds through the C5 pathway from glutamate, a direct derivative of the tricarboxylic acid (TCA) cycle. This process requires glutamyl-tRNA synthetase (GluRS), glutamyl-tRNA reductase (HemA) and glutamate-1-semialdehyde aminotransferase (HemL). Although the complete genomic DNA sequence of Nissle 1917 is deposited in GenBank (accession number CP007799) (Reister *et al.*, 2014), these three enzymes from Nissle 1917 are unannotated. We therefore cloned Nissle 1917 *gltX*, *hemA* and *hemL* genes with specific primers designed from *E. coli* MG1655 to confirm the C5 pathway of Nissle 1917. The amino acid sequences encoded by Nissle 1917 *gltX*, *hemA* and *hemL* genes are 99.58%, 98.09% and 99.30% identical to their respective cognate counterparts in *E. coli* MG1655 (Fig. S1). Their GenBank accession numbers were, respectively, annotated as MW504637, MW504638 and MW504639. These high sequence identities suggested that these cloned Nissle 1917 *gltX*, *hemA* and *hemL* genes encode glutamyl-tRNA synthetase, glutamyl-tRNA reductase and glutamate-1-semialdehyde aminotransferase, respectively.

Nissle 1917 possesses two small cryptic plasmids, pMUT1 and pMUT2 (Yu *et al.*, 2020). The former carries a ColE1-type-replication system, which is present in the high copy-number plasmid pUC19. To avoid genetic instability, we chose the low copy-number plasmid pCL1920 to overexpress *gltX*, *hemA* and *hemL* in Nissle 1917 (designated strains ENX, ENA and ENL, respectively). Only ENA produced increased levels of 5-ALA, ENX produced lower levels of 5-ALA accumulation, and ENL accumulated 5-ALA similarly to EN1920, containing pCL1920 as control (Table 1).

Table 1. 5-ALA production by recombinant Nissle 1917 expressing genes encoding components of the 5-ALA biosynthetic pathway. A 2% (v/v) inoculum from an overnight culture for 12 h was used.

Nissle 1917 strains	Expressed genes	Cell biomass (OD_{600})	5-ALA accumulation (mg l^{-1})
EN1920	–	8.26 ± 0.57	21.43 ± 1.74
ENX	*gltX*	8.03 ± 0.68	17.64 ± 1.35
ENA	*hemA*	7.89 ± 0.64	31.85 ± 3.64
ENL	*hemL*	7.94 ± 0.71	24.37 ± 2.75
EAL	*hemA* and *hemL*	8.15 ± 0.75	42.62 ± 3.87*
ENAL	*hemA*^{M} and *hemL*	7.26 ± 0.52	194.33 ± 18.63 **

Samples were taken and measured until 48 h. 20 g l^{-1} glucose was added initially as sole carbon source. The results represent the data of three individual experiments (*$P < 0.05$, **$P < 0.01$, two-way ANOVA with Dunnett's multiple comparisons test, mean ± SEM).

The coexpression of endogenous *hemA* and *hemL* further improved 5-ALA accumulation compared with that of EN1920 (Table 1). These results indicated that the conversion of glutamyl-tRNA to glutamate-1-semialdehyde catalysed by HemA is likely a rate-limiting step. The activity of HemA may be upregulated to increase 5-ALA production in Nissle 1917. Meanwhile, researchers found that HemA is not stable to be proteolytic, and its stability is significantly increased by inserting two lysines (codons: AAGAAG) between Thr-2 and Leu-3 at N terminus of the protein. Therefore, we made the same mutation with the HemA from *Salmonella arizona* to generate HemA^M. The coexpression of *S. arizona hemA*^{M} with endogenous *hemL* in Nissle 1917 greatly increased 5-ALA accumulation (194 mg l^{-1}). This will be beneficial to the metabolic production of 5-ALA in Nissle 1917.

Inhibition of downstream pathway to enhance 5-ALA production

Levulinic acid (LA) is used to inhibit the downstream biosynthetic pathway of 5-ALA to enhance its production in *Corynebacterium glutamicum* (Yu *et al.*, 2015). Here, addition of LA in Nissle 1917 ENAL did not influence its growth and glucose consumption (Fig. 2A and B), while increasing 5-ALA production and decreasing the accumulation of porphobilinogen (PBG). 5-ALA production gradually increased when cells were treated with 0.5 to 2 mM LA and reached 300 mg l^{-1} in the presence of 1 mM LA (Fig. 2C). Compared with the control, the accumulation of PBG was significantly lower in the presence of LA (0.5–2 mM) (Fig. 2D). The colour of the culture medium lightened in the presence of higher concentrations of LA, indicating the reduction in the levels of porphyrins and haeme (Fig. 2E). These results suggested that the inhibition of downstream metabolic pathway

components affected cell metabolism and increased 5-ALA production to levels sufficient for therapeutic applications.

Analysis of engineered Nissle 1917 ENAL *in vitro*

We firstly evaluated the therapeutic potential of engineered Nissle 1917 using the human colorectal cancer cell line HCT116. ENAL cultured in the presence of 1 mM LA for 24 h was chosen to inoculate HCT116 cells to determine whether enhanced PpIX accumulation is a common phenomenon among exogenous 5-ALA·HCl and ENAL. As shown in Fig. 3A, 5-ALA·HCl significantly enhanced PpIX fluorescence in a concentration-dependent manner. The PpIX fluorescence was also increased compared with control when HCT116 cells were exposed to ENAL for 90 min. We found that ENAL-induced PpIX fluorescence was similar to a 5-ALA·HCl concentration of 40 mg l^{-1}. These results demonstrate that ENAL efficiently and selectively enhanced PpIX fluorescence within tumours *in vitro*.

The cytotoxicity of ENAL and different concentrations of 5-ALA·HCl were evaluated using an MTT assay after HCT116 cells were irradiated with 660 nm light. We found that a high concentration of 5-ALA·HCl effectively induced cell death. Treatment with ENAL for 90 min decreased cell viability more potently than control and showed almost the same effect as 20 or 40 mg l^{-1} 5-ALA·HCl (Fig. 3B). These results suggested that ENAL, through production of 5-ALA, increased PpIX fluorescence to inhibit the viability of HCT116 cells.

We next used the fluorescence probe 2,7-dichlorodihydrofluorescein diacetate (DCFH-DA) to further measure ROS generation induced by PpIX in irradiated HCT116 cells treated with 5-ALA·HCl and ENAL. As shown in Fig. 3C, the intracellular ROS levels increased with the addition of different amounts of 5-ALA·HCl for 8 h. ENAL, treated for 90 min, significantly induced intracellular ROS levels upon irradiation compared with controls. ENAL and 5-ALA·HCl generated nearly the same amount of ROS. These findings indicated that ENAL with production of 5-ALA could enhance ROS generation in tumour cells leading to increased apoptosis.

Nissle 1917 ENAL inhibited tumour growth *in vivo*

To further demonstrate the antitumour activity of Nissle 1917 ENAL, HCT116 cells were subcutaneously injected into Balb/c mice to establish tumour xenograft. When the tumour grew to approximately 0.2 cm^3, the mice were given PBS, EN1920, 5-ALA·HCl (20, 50 mg kg^{-1}) or ENAL by intraperitoneal (i.p.) injection. EN1920 and
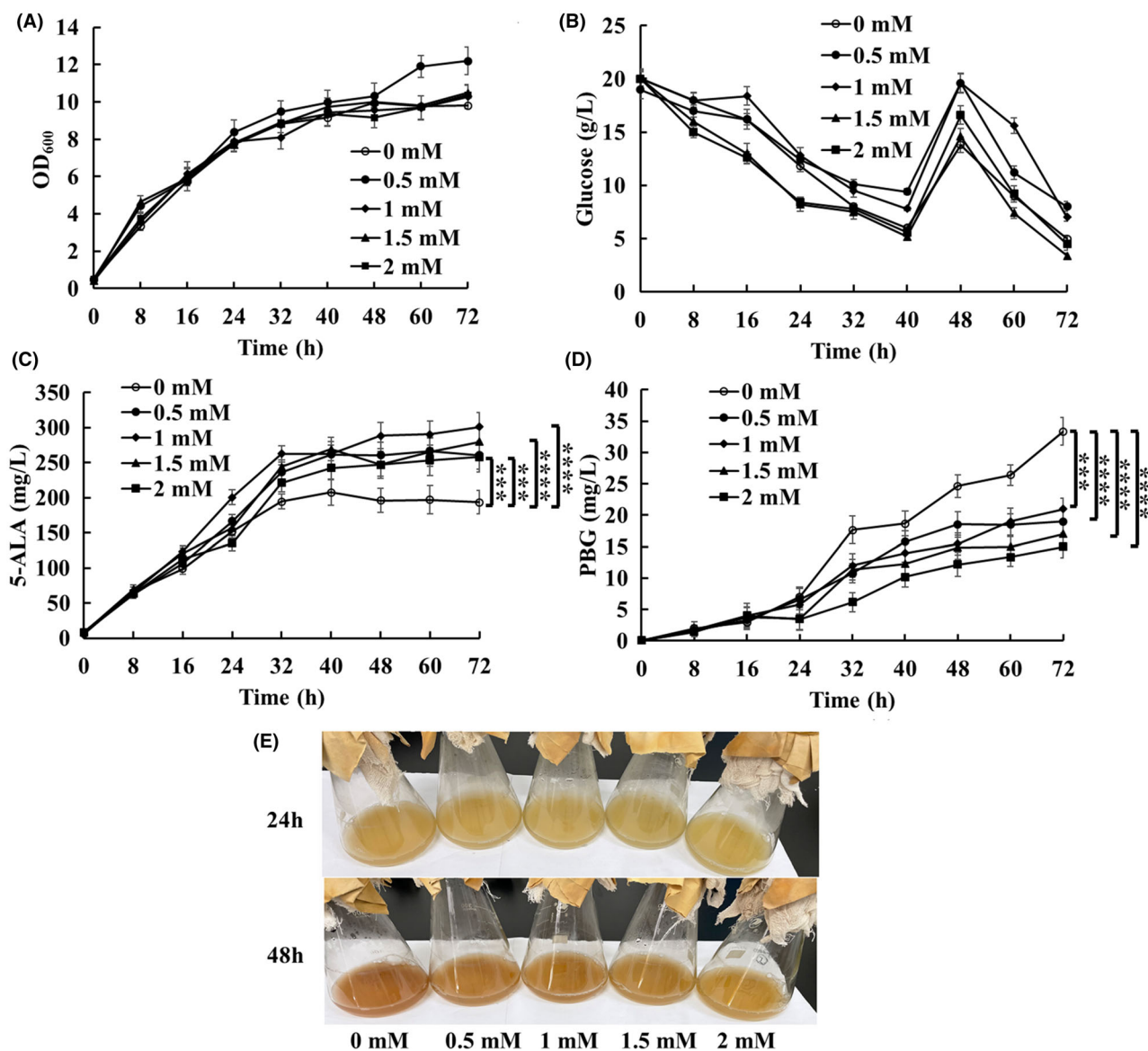
Fig. 2. The growth (A), glucose consumption (B), accumulation of 5-ALA (C) and PBG (D) and colour changes (E) in Nissle 1917 ENAL after addition of LA. 20 g l^{-1} glucose was added initially as the sole carbon source with 10 g l^{-1} addition at 40 h. Statistical analysis was conducted using two-way ANOVA with Tukey's multiple comparisons test, ***$P < 0.001$, ****$P < 0.0001$ ($n = 3$ per group; each group tested in triplicate; mean ± SEM).

ENAL were administered at a dose of 1×10^7 CFU per mouse. ENAL targeted the tumour site but not normal tissues such as the kidneys, liver, heart and spleen (Fig. 4A). The number of bacteria in tumours reached 10^9 CFU g^{-1} and remained at this level for approximately 8 days.

ENAL (1×10^7 CFU) inhibited the growth of tumours formed by HCT116 cells by 50.1% and significantly delayed tumour growth compared with the PBS control (Fig. 4B and C). The growth of the group receiving EN1920 was not significantly different compared with that of the PBS group, indicating that the

parental Nissle 1917 strain was insufficient to prevent tumour growth individually. The mean tumour size in mice administered 20 or 50 mg kg^{-1} 5-ALA·HCl was significantly reduced. ENAL achieved better therapeutic efficacy than treatment with 20 mg kg^{-1} 5-ALA·HCl.

Furthermore, the body weights of all treatment groups were not affected, suggesting that bacterial therapy was well-tolerated (Fig. 4D). These results indicated that ENAL caused a cytotoxic effect in tumour xenografts through the production of 5-ALA without detectable toxicity to normal tissues.

Discussion

In this study, we engineered the probiotic Nissle 1917 to efficiently produce 5-ALA and employed Nissle 1917 as a drug carrier to deliver 5-ALA for cancer therapy. 5-ALA biosynthesis is the focus of numerous investigations because of its potential applications in the PDT of cancers. For example, Nissle 1917 is prescribed for use in humans, and clinical trials established its safety when used to prevent inflammatory bowel disease (Schultz, 2008). Similarly, clinical trials demonstrate the safety of attenuated *S. typhimurium* (Toso *et al.*, 2002), although this finding has not yet been extended to engineered microbes.

We firstly identified the three key Nissle 1917 genes predicted to encode enzymes that mediate 5-ALA biosynthesis. The results showed that the reduction in glutamyl-tRNA to glutamate-1-semialdehyde, catalysed by HemA, is possibly a rate-limiting step. Previous studies determined that HemA is a major control point for 5-ALA biosynthesis (Kang *et al.*, 2011). However, HemA from *S. typhimurium* is unstable, and its stability is greatly decreased in unrestricted cells or when haeme is accumulated (Wang *et al.*, 1999a). Due to the instability of HemA to proteolysis, it is difficult to overproduce *S. typhimurium* HemA using the tac promoter or T7 RNA polymerase-directed systems (Wang *et al.*, 1999b). However, the stability of HemA in *S. typhimurium* is
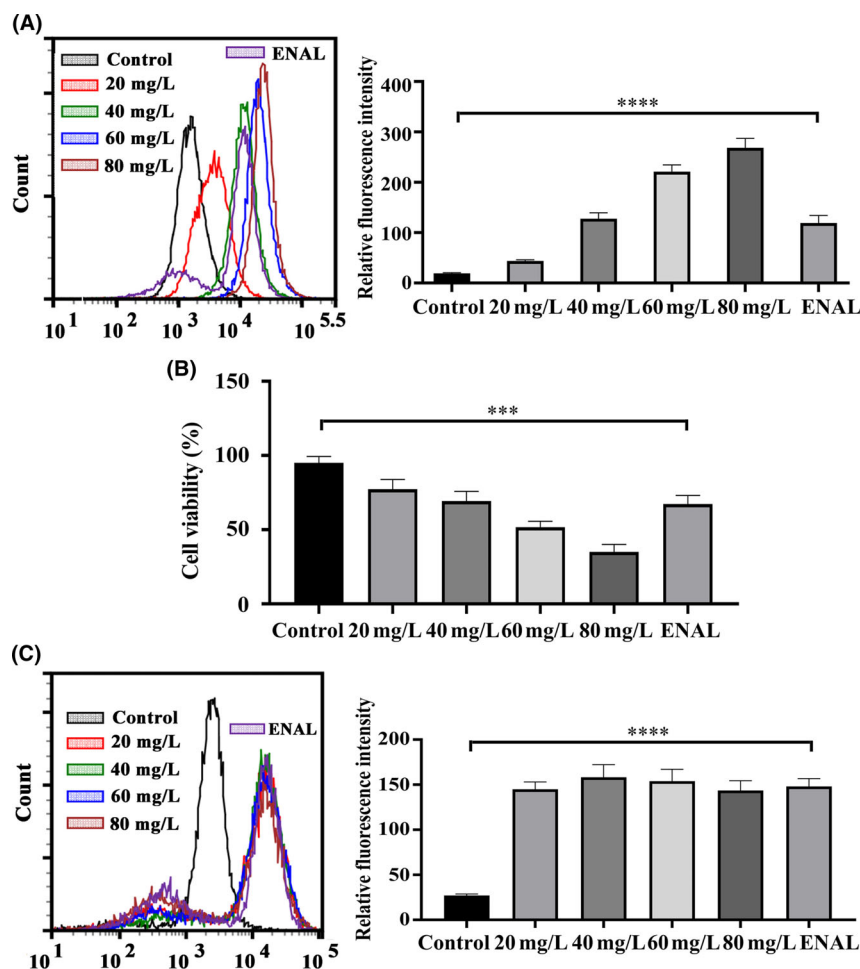

Fig. 3. *In vitro* analysis of the anticancer effects of 5-ALA·HCl and Nissle 1917 ENAL.
A. Representative histogram (left) and bar graph (right) of PpIX fluorescence measured by flow cytometry in HCT116 cells treated with 5-ALA·HCl for 6 h and with ENAL for 90 min ($n = 3$ per group of three replicates, ****$P < 0.0001$, two-way ANOVA with Dunnett's multiple comparisons test).
B. Cell viability assay of the *in vitro* anticancer effects of 5-ALA·HCl and ENAL ($n = 3$ per group of three replicates, ***$P < 0.001$, two-way ANOVA with Dunnett's multiple comparisons test).
C. DCFH-DA assay (representative histogram and bar graph) of intracellular ROS generation using flow cytometry of HCT116 cells treated with 5-ALA·HCl for 8 h and with ENAL for 90 min ($n = 3$ per group of three replicates, ****$P < 0.0001$, two-way ANOVA with Dunnett's multiple comparisons test). All data are expressed as the mean ± SEM.
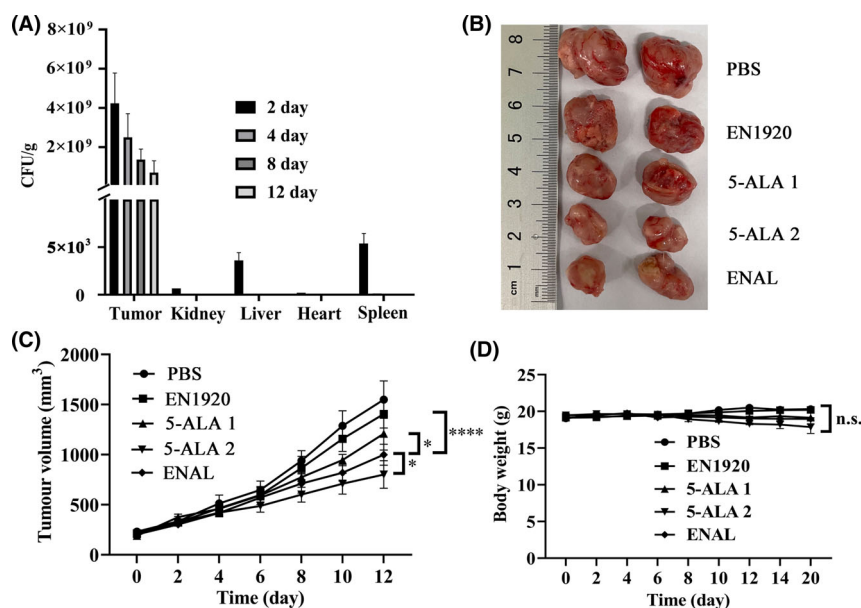
Fig. 4. Treatment with 5-ALA·HCl and Nissle 1917 ENAL reduces the tumour growth rate in a xenograft model.
A. The retention of ENAL in different tissues was measured on days 2 ($n = 4$ mice), 4 ($n = 3$ mice), 8 ($n = 3$ mice) and 12 ($n = 4$ mice) after i.p. administration of 1×10^7 CFU.
B–C. Mice transplanted with HCT116 cells were treated daily for 12 days with PBS, ALA 1 (20 mg kg^{-1} 5-ALA·HCl), ALA 2 (50 mg kg^{-1} 5-ALA·HCl); or treated with 1×10^7 cells 100 μl^{-1} PBS of EN1920 or ENAL every six days for 12 days ($n = 3–4$ per group, $*P = 0.0227$, $*P = 0.0457$, $****P < 0.0001$, two-way ANOVA with Dunnett's multiple comparisons test).
D. Body weight of each group ($n = 3–4$ per group, n.s. not significant ($P > 0.05$), two-way ANOVA with Dunnett's multiple comparisons test). All data are shown as mean ± SEM.

significantly increased by inserting two lysines (codons: AAGAAG) between Thr-2 and Leu-3 at N terminus of the protein (Kang *et al.*, 2011). Thus, HemA^M from *S. arizona*, inserted two lysine residues, was generated. The amino acid sequence of *hemA* from *S. arizona* is identical to that from *S. typhimurium*. We therefore used the *hemA* gene from *S. arizona* instead. The coexpression of *hemA*^{M} with Nissle 1917 *hemL* produced the highest level of 5-ALA, indicating that these two enzymes synergized through the formation of a tight complex, consistent with findings that HemL forms such a complex with HemA in *E. coli* by co-immunoprecipitation experiments and gel permeation chromatography (Luer *et al.*, 2005). The similarity of the amino acid sequence of HemA from Nissle 1917 and HemA^M from *S. arizona* was 98%. Therefore, complex formation between the highly stable and active HemA^M from *S. arizona* and HemL from Nissle 1917 indicated the efficient and quick transfer of glutamate-1-semialdehyde aminotransferase (GSA), leading to high accumulation of ALA in strain ENAL.

To further increase 5-ALA production, the downstream metabolic pathway of 5-ALA should be inhibited. A *hemB* mutant of *E. coli* does not produce higher levels of 5-ALA compared with wild type (Xie *et al.*, 2003). However, addition of a competitive inhibitor such as LA considerably inhibits the expression of ALAD (encoded by

hemB gene) to increase 5-ALA production by *C. glutamicum* (Yu *et al.*, 2015), *R. sphaeroides* (Nishikawa *et al.*, 1999) and *Chlorella vulgaris* (Ano *et al.*, 2000). In Nissle 1917 ENAL, LA increases 5-ALA production with a decrease in the accumulation of PBG. It has been demonstrated that 15 mM LA inhibits ALAD activity by 60% at pH 6.5 (Nishikawa *et al.*, 1999). Consequently, LA with inhibitory activities likely affects distinct steps of the reaction mechanism to influence the kinetics of the ALAD reactions (Jarret *et al.*, 2000). Thus, LA efficiently inhibited ALAD activity to increase the production of 5-ALA in Nissle 1917.

Nissle 1917 with production of 5-ALA may be applied to deliver 5-ALA to target tumours as a living delivery system. Compared with 5-ALA·HCl, engineered ENAL increased PpIX accumulation and decreased cell viability. It is known that 5-ALA treatment induces PpIX accumulation more efficiently in cancer cells because of their high metabolic activity and activated haeme biosynthetic pathway (Fujino *et al.*, 2016). Cellular PpIX concentration indicates a function of the rate of metabolic conversion of 5-ALA (Yang *et al.*, 2015). The higher level of PpIX in HCT116 cells infected with ENAL provides evidence that Nissle 1917 produced and delivered 5-ALA to cancer cells *in vitro*. The delivery of 5-ALA increased the haeme biosynthesis of cancer cells to form PpIX. After

irradiation of HCT116 cells infected with ENAL, cytotoxi-city and ROS generation were enhanced. These results indicated that ENAL caused irradiated tumour cells to undergo apoptosis through the generation of ROS.

To further verify the effects of this living delivery system *in vivo*, Nissle 1917 ENAL was injected into tumour-bearing mice, resulting in smaller tumours compared with controls. Considerable numbers of ENAL were detected at the tumour sites, partially avoiding damage to normal tissues. It has been reported that the inflammatory microenvironment is the driving force for tumour targeting (Zheng *et al.*, 2018). One mechanism of Nissle 1917-mediated tumour targeting occurs after inflammation (Yu *et al.*, 2020). For example, Zhang *et al.*, (2012) demonstrated the safety and efficiency of Nissle 1917 in mice. Tumour growth and pulmonary metastasis are efficiently suppressed by azurin release, and the resulting inflammatory response does not cause significant toxicity (Zhang *et al.*, 2012). Tumour-targeted lymphocytes (Zheng *et al.*, 2018) or matrix metalloproteinase-2 (MMP-2) and pH dual-sensitive nanocarriers (Wu *et al.*, 2017) deliver 5-ALA that specifically accumulates within cancer cells to generate PpIX and induce photodynamic cytotoxicity. Nissle 1917 may therefore represent an alternative delivery system for targeted photodynamic cancer therapy. In contrast to *Salmonella* and *Clostridium novyi* NT, which have been extensively investigated as vehicles for antitumour drugs (Agrawal *et al.*, 2004), Nissle 1917 has high tumour-targeting capability and rapidly release drugs such as 5-ALA to cancer cells.

Although the concept of microbial synthesis and secretion of anticancer compounds is an attractive option for targeted drug delivery, limitations remain. The genetic instability, cell count-dependent and undefined dosage of the cell-synthesized 5-ALA, and 5-ALA bioavailability for PpIX synthesis in cancer cells are important and interesting issues.

In summary, we combined the biosynthetic and tumour-targeting features of probiotic Nissle 1917 with PDT to inhibit the growth of colorectal cancer cells. Thus, genetically engineered Nissle 1917 produced and delivered 5-ALA for cancer therapy. This study contributes an alternative strategy for constructing delivery systems for bacteriolytic cancer therapy.

Experimental procedures

Bacterial strains, primers and plasmids

All strains, plasmids and oligonucleotides used in this study are summarized in the additional files (Tables S1 and S2). The *gltX*, *hemA* and *hemL* genes were cloned from the genome of Nissle 1917 using primers gltx-F, gltx-R and hema-F, hema-R, and heml-F, and heml-R, respectively. These three amplicons were ligated into

pCL1920, which was digested with *Bam*HI (Fermentas, Shanghai, China) according to the method of Gibson assembly. Molecular cloning and manipulation of plasmids were performed with *E. coli* DH5α. To increase the stability of HemA, *hemA* was amplified from the *S. arizona* genome, which encodes the same predicted HemA amino acid sequence of *S. typhimurium* using primers hemA^M-F and hemA^M-R. The primer hemA^M-F was inserted with two codons (AAGAAG) encoding Lys between Thr-2 and Leu-3 at the N terminus to generate *hemA^M* (Wang *et al.*, 1999a). The *hemL* gene was amplified using the primers theml-F and heml-R and ligated together with *hemA^M* into pCL1920. The sequences of the plasmids were verified by the BioSune Company (Shanghai, China). Nissle 1917 was used as parental strain for 5-ALA production.

Media, culture conditions and analytical procedures

LB medium (10 g l^{-1} tryptone, 5 g l^{-1} yeast extract and 10 g l^{-1} NaCl, pH 7.2) was used for molecular genetic procedures. The modified minimal medium, which contains 16 g l^{-1} $(NH4)_2SO_4$, 3 g l^{-1} KH_2PO_4, 16 g l^{-1} $Na_2HPO_4 \cdot 12H_2O$, 1 g l^{-1} $MgSO_4 \cdot 7H_2O$, 0.01 g l^{-1} $MnSO_4 \cdot 7H_2O$ and 2 g l^{-1} yeast extract, was used for cultivation and fermentation. Glucose was as sole carbon source, and spectinomycin (25 mg ml^{-1}) was used for selecting mutants. To induce the expression of plasmid genes, isopropyl-β-d-thiogalactopyranoside (IPTG) was added to the cultures at a final concentration of 0.1 mM.

5-ALA was produced at 37°C in 300 ml using ordinary flasks containing 50 ml modified minimal medium with agitation of 240 rpm. 20 g l^{-1} glucose was added initially as the sole carbon source. The initial pH was adjusted to 7.0 and then maintained at approximately pH 6.5 using 4 M NaOH. The inhibitor LA was added at the initial stage.

The OD_{600} was determined using a spectrophotometer (Shimadzu, Japan), and the supernatant was analysed for glucose using SBA-40C biosensor (developed by Biology Institute of Shandong Academy of Sciences) equipped with glucose oxidase immobilized on membranes. The supernatant was also used for 5-ALA analysis using modified Ehrlich's reagent (Yu *et al.*, 2015).

Cell lines and animal models

HCT116 cells, which were purchased from the Cell Bank of Shanghai Institute of Cell Biology, Chinese Academy of Sciences (Shanghai, China), were maintained in a DMEM medium containing 10% fetal bovine serum (FBS), 100 mg ml^{-1} penicillin and 100 U ml^{-1} streptomycin, in a humidified incubator at 37°C in an atmosphere of 5% CO_2.

Animal experiments were performed according to the guidelines for laboratory animals established by the Weifang Medical University Center for Animal Center Experiment. Female Balb/c mice (5–6 weeks of age) were purchased from Ji'nan Pengyue Laboratory Animal Breeding Co., Ltd. (Jinan, China). Mice were bred and maintained under specific-pathogen-free (SPF) conditions for at least 3 days before use. HCT116 cells (1×10^6 100 μl^{-1}) were subcutaneously inoculated into mice on the mid-right side. When tumours reached a mean group volume of approximately 0.2 cm^3, mice were randomly divided into the groups as follows: PBS, 5-ALA·HCl (20 or 50 mg kg^{-1}), EN1920 and ENAL. Tumour volume = (length $\times$ width^2)/2.

PpIX measurement

HCT116 cells were added to 24-well tissue culture plates (approximately 10^5 cells per well) and cultured for 24 h at 37°C in an atmosphere containing 5% CO_2. Different concentrations of 5-ALA·HCl (Solarbio, Beijing, China) were prepared using DMEM. Each well was treated with 1 ml of diluted 5-ALA·HCl for 6 h before measuring the PpIX concentration. The fermentation broth used to culture ENAL for 24 h was centrifuged at 4000 $\times$ g for 3 min, and the pelleted cells were washed with PBS and resuspended in DMEM to 3×10^7 CFU ml^{-1}. $OD_{600} = 1.0$ of statically grown cultures was equivalent to approximately 3×10^8 CFU ml^{-1}. ENAL was resuspended in 1 ml of DMEM and added to a single well at multiplicity of infection (MOI) of 300:1. After 90 min of infection at 37°C, the wells were washed five times with 1 ml of PBS at room temperature. Then, the cells were used for PpIX measurement. PBS served as the control, and PpIX fluorescence was measured using flow cytometry (488 nm excitation/650 nm emission; ACEA Biosciences Inc., Hangzhou, China).

Cell viability assays

HCT116 cells (approximately 3000 cells per well) were added to 96-well plates for 24 h and subsequently treated with different concentrations of 5-ALA·HCl for 12 h. ENAL was cultured and harvested as described above and then resuspended in DMEM to 1×10^7 CFU ml^{-1}. Resuspended ENAL (100 μl) was added and incubated for 90 min. Controls were cultured under the same conditions with PBS. Treated cells were irradiated for 5 min (660 nm LED light, 29.8 mW cm^{-2}). After incubation for 24 h, cell viability was determined using an MTT assay.

ROS detection by DCFH-DA

Flow cytometry (488 nm excitation/525 nm) using DCFH-DA (Sigma, Shanghai, China) was used to measure the generation of ROS produced by PpIX in irradiated cells. First, $\sim 10^5$ HCT116 cells/well were seeded into 24-well tissue culture plates for 24 h and incubated with different amounts of 5-ALA·HCl for 8 h or with ENAL at a MOI of 300:1 for 90 min, respectively. PBS served as a negative control. Samples of cells were subsequently illuminated for 5 min (660 nm LED light, 29.8 mW cm^{-2}). After 2 h of cultivation, DMEM containing 10 μM DCFH-DA was added into wells and incubated for 20 min at 37°C. Finally, cells were washed three times with PBS and then analysed as soon as possible.

Infection of tumour-bearing mice

PBS, 20 or 50 mg kg^{-1} 5-ALA·HCl was intraperitoneally injected into tumour-bearing mice once each day for 12 days. EN1920 and ENAL were cultured as described above and resuspended in sterile PBS at 1×10^8 CFU ml^{-1}. The number of CFUs was determined for each independent experiment (experimental error $< 10\%$). This bacterial stock (1×10^7 CFU in 100 μl PBS) of EN1920 and ENAL was, respectively, used to intraperitoneally inoculate tumour-bearing mice every six days for 12 days. These bacterial doses showed normal phenotype such as mobility and weight throughout the entire experiment. In contrast, most mice died after injection with higher doses of bacteria. The mice infected with EN1920 and ENAL were provided with 0.5% glucose and 25 mg ml^{-1} spectinomycin in their drinking water, which was changed every 2–3 days. Mice were intraperitoneally injected with freshly prepared IPTG or LA (1 mg 200 μl^{-1}). After treatment for 24 h, the dose of light irradiation for 5 min (660 nm, 150 mW cm^{-2}) was administered to the members of each group. Then, tumour volumes and the body weights were measured and recorded every 2 days. The relative tumour volume and body weight were compared with those measured on the first day.

Mice were killed to measure the CFU g^{-1} of tumours, liver, heart and spleens. Tumours were excised, placed into sterile tubes containing 5 ml of PBS, weighed and homogenized by soft mechanical squeezing. Next, 100 μl of a homogenate was serially diluted in LB, plated on LB agar containing spectinomycin and incubated overnight at 37°C. Bacterial titres are expressed as CFU g^{-1} of tissue.

Statistical analysis and sample collection

Two-way ANOVA with Tukey's or Dunnett's multiple comparisons test was performed using GraphPad Prism 8 (GraphPad Software, La Jolla, CA, USA). Investigators performing operations were blinded to treatment groups in cell experiments and *in vivo* experiments. For *in vivo*

experiments, mice were randomly divided into different groups.

Conflict of interest

None declared.

References

Agrawal, N., Bettegowda, C., Cheong, I., Geschwind, J.F., Drake, C.G., Hipkiss, E.L., *et al.* (2004) Bacteriolytic therapy can generate a potent immune response against experimental tumors. *Proc Natl Acad Sci USA* **101:** 15172–15177.

Ano, A., Funahashi, H., Nakao, K., and Nishizawa, Y. (2000) Effects of levulinic acid on 5-aminolevulinic acid production in heterotrophic cultures of *Chlorella regularis* YA-603. *J Biosci Bioeng* **89:** 176–180.

Bray, F., Ferlay, J., Soerjomataram, I., Siegel, R.L., Torre, L.A., and Jemal, A. (2018) Global cancer statistics 2018: GLOBOCAN estimates of incidence and mortality worldwide for 36 cancers in 185 countries. *CA Cancer J Clin* **68:** 394–424.

Chowdhury, S., Castro, S., Coker, C., Hinchliffe, T.E., Arpaia, N., and Danino, T. (2019) Programmable bacteria induce durable tumor regression and systemic antitumor immunity. *Nat Med* **25:** 1057–1063.

Chua, K.J., Kwok, W.C., Aggarwal, N., Sun, T., and Chang, M.W. (2017) Designer probiotics for the prevention and treatment of human diseases. *Curr Opin Chem Biol* **40:** 8–16.

Donnelly, R.F., McCarron, P.A., and Woolfson, A.D. (2008) Derivatives of 5-aminolevulinic acid for photodynamic therapy. *Perspect Medicin Chem* **1:** 49–63.

Dougherty, T.J., Gomer, C.J., Henderson, B.W., Jori, G., Kessel, D., Korbelik, M., *et al.* (1998) Photodynamic therapy. *J Natl Cancer Inst* **90:** 889–905.

Forbes, N.S. (2010) Engineering the perfect (bacterial) cancer therapy. *Nat Rev Cancer* **10:** 785–794.

Fujino, M., Nishio, Y., Ito, H., Tanaka, T., and Li, X.K. (2016) 5-Aminolevulinic acid regulates the inflammatory response and alloimmune reaction. *Int Immunopharmacol* **37:** 71–78.

Hill, C., Guarner, F., Reid, G., Gibson, G.R., Merenstein, D.J., Pot, B., *et al.* (2014) Expert consensus document. The International Scientific Association for Probiotics and Prebiotics consensus statement on the scope and appropriate use of the term probiotic. *Nat Rev Gastroenterol Hepatol* **11:** 506–514.

Jarret, C., Stauffer, F., Henz, M.E., Marty, M., Lüönd, R.M., Bobálová, J., *et al.* (2000) Inhibition of *Escherichia coli* porphobilinogen synthase using analogs of postulated intermediates. *Chem Biol* **7:** 185–196.

Kang, Z., Wang, Y., Gu, P., Wang, Q., and Qi, Q. (2011) Engineering *Escherichia coli* for efficient production of 5-aminolevulinic acid from glucose. *Metab Eng* **13:** 492–849.

Kim, C.H., Chung, C.W., Lee, H.M., Kim, D.H., Kwak, T.W., Jeong, Y.I., and Kang, D.H. (2013) Synergistic effects of 5-aminolevulinic acid based photodynamic therapy and celecoxib via oxidative stress in human cholangiocarcinoma cells. *Int J Nanomedicine* **8:** 2173–2186.

Luer, C., Schauer, S., Mobius, K., Schulze, J., Schubert, W.D., Heinz, D.W., *et al.* (2005) Complex formation between glutamyl-tRNA reductase and glutamate-1-semialdehyde 2,1-aminomutase in *Escherichia coli* during the initial reactions of porphyrin biosynthesis. *J Biol Chem* **280:** 18568–18572.

Nishikawa, S., Watanabe, K., Tanaka, T., Miyachi, N., Hotta, Y., and Murooka, Y. (1999) *Rhodobacter sphaeroides* mutants which accumulate 5-aminolevulinic acid under aerobic and dark conditions. *J Biosci Bioeng* **87:** 798–804.

Pedrolli, D.B., Ribeiro, N.V., Squizato, P.N., de Jesus, V.N., Cozetto, D.A., Tuma, R.B., *et al.* Team AQA Unesp at iGEM 2017. (2019) Engineering microbial living therapeutics: the synthetic biology toolbox. *Trends Biotechnol* **37:** 100–115.

Piñero-Lambea, C., Bodelón, G., Fernández-Periáñez, R., Cuesta, A.M., Álvarez-Vallina, L., and Fernández, L.Á. (2015) Programming controlled adhesion of *E. coli* to target surfaces, cells, and tumors with synthetic adhesins. *ACS Synth Biol* **4:** 463–473.

Reister, M., Hoffmeier, K., Krezdorn, N., Rotter, B., Liang, C., Rund, S., *et al.* (2014) Complete genome sequence of the gram-negative probiotic *Escherichia coli* strain Nissle 1917. *J Biotechnol* **187:** 106–107.

Schauer, S., Chaturvedi, S., Randau, L., Moser, J., Kitabatake, M., Lorenz, S., *et al.* (2002) *Escherichia coli* glutamyl-tRNA reductase. Trapping the thioester intermediate. *J Biol Chem* **277:** 48657–48663.

Schultz, M. (2008) Clinical use of *E. coli* Nissle 1917 in inflammatory bowel disease. *Inflamm Bowel Dis* **14:** 1012–1018.

Sharma, S., Jajoo, A., and Dube, A. (2007) 5-Aminolevulinic acid-induced protoporphyrin-IX accumulation and associated phototoxicity in macrophages and oral cancer cell lines. *J Photochem Photobiol B* **88:** 156–162.

Singh, B., Mal, G., and Marotta, F. (2017) Designer probiotics: paving the way to living therapeutics. *Trends Biotechnol* **35:** 679–682.

Toso, J.F., Gill, V.J., Hwu, P., Marincola, F.M., Restifo, N.P., Schwartzentruber, D.J., *et al*. (2002) Phase I study of the intravenous administration of attenuated *Salmonella typhimurium* to patients with metastatic melanoma. *J Clin Oncol* **20:** 142–152.

Wang, L., Elliott, M., and Elliott, T. (1999a) Conditional stability of the HemA protein (glutamyl-tRNA reductase) regulates heme biosynthesis in *Salmonella typhimurium*. *J Bacteriol* **181:** 1211–1219.

Wang, L., Wilson, S., and Elliott, T. (1999b) A mutant HemA protein with positive charge close to the N terminus is stabilized against heme-regulated proteolysis in *Salmonella typhimurium*. *J Bacteriol* **181:** 6033–6041.

Woźniak, M., Duś-Szachniewicz, K., and Ziółkowski, P. (2015) Insulin-like growth factor-2 is induced following 5-aminolevulinic acid-mediated photodynamic therapy in SW620 human colon cancer cell line. *Int J Mol Sci* **16:** 23615–23629.

Wu, J., Han, H., Jin, Q., Li, Z., Li, H., and Ji, J. (2017) Design and proof of programmed 5-aminolevulinic acid prodrug nanocarriers for targeted photodynamic cancer therapy. *ACS Appl Mater Interfaces* **9:** 14596–14605.

Xie, L., Eiteman, M.A., and Altman, E. (2003) Production of 5-aminolevulinic acid by an *Escherichia coli* aminolevulinate dehydratase mutant that overproduces *Rhodobacter sphaeroides* aminolevulinate synthase. *Biotechnol Lett* **25:** 1751–1755.

Yang, S.J., Shieh, M.J., Lin, F.H., Lou, P.J., Peng, C.L., Wei, M.F., *et al*. (2009) Colorectal cancer cell detection by 5-aminolaevulinic acid-loaded chitosan nano-particles. *Cancer Lett* **273:** 210–220.

Yang, X., Palasuberniam, P., Kraus, D., and Chen, B. (2015) Aminolevulinic acid-based tumor detection and therapy: molecular mechanisms and strategies for enhancement. *Int J Mol Sci* **16:** 25865–25880.

Yu, X., Jin, H., Liu, W., Wang, Q., and Qi, Q. (2015) Engineering *Corynebacterium glutamicum* to produce 5-aminolevulinic acid from glucose. *Microb Cell Fact* **14:** 183.

Yu, X., Lin, C., Yu, J., Qi, Q., and Wang, Q. (2020) Bioengineered *Escherichia coli* Nissle 1917 for tumour-targeting therapy. *Microb Biotechnol* **13:** 629–636.

Zhang, Y., Zhang, Y., Xia, L., Zhang, X., Ding, X., Yan, F., and Wu, F. (2012) *Escherichia coli* Nissle 1917 targets and restrains mouse B16 melanoma and 4T1 breast tumors through expression of azurin protein. *Appl Environ Microbiol* **78:** 7603–7610.

Zheng, D.W., Fan, J.X., Liu, X.H., Dong, X., Pan, P., Xu, L., and Zhang, X.Z. (2018) A simply modified lymphocyte for systematic cancer therapy. *Adv Mater* **30:** e1801622.

Supporting information

Additional supporting information may be found online in the Supporting Information section at the end of the article.

Fig. S1. The homology of GluRS, HemA and HemL between *E. coli* MG1655 and *E. coli* Nissle 1917.

Table S1. Strains and plasmids used in this study.

Table S2. Primers used in this study.